Measurements of Turbulent Micro-Structure in Bubbly Flows Using Combined PIV/LIF/IST Technique

Koichi HISHDA*, Akiko FUJIWARA*,
Shigeaki NAGAYA**, Akira KAKUGAWA**, and Yoshiaki KODAMA**
**Department of System Design Engineering, Keio University,*
3-14-1 Hiyoshi Kohoku-ku Yokohama, 223-8522, Japan
***Turbulence Control Group, Ship Research Institute,*
6-38-1 Shinkawa Mitaka, Tokyo 181-0004, Japan

Experimental studies have been performed on turbulent microstructures in a simple shear layer flow involving a single rising bubble, an upward bubbly channel flow and microbubbles water channel flow for skin friction reduction. Velocity measurements were made using one digital high-speed CCD camera for Digital Particle Image Velocimetry (DPIV) with fluorescent tracer particles (PIV/LIF). The recorded image data were analyzed by cross-correlation technique. A second CCD camera was used to detect the bubble's shape and translational motion via backlighting from a square array of infrared LED's (Infrared Shadow Technique IST). We clarified turbulent structures of surrounding fluid that was influenced by the bubble motion, quantitatively measured by PIV/LIF/IST technique.

1. Introduction

One of the most important aspects of dispersed two-phase flow is the interaction of dispersed phase with turbulent flow, which controls the performance of many engineering devices. In gas-liquid two-phase flow many experimental evidence indicated that the turbulent intensity became decreased, while it became increased according to dependence on the void fraction and gas flow rate (Serizawa et al., 1975, Theofanous and Sullivan, 1982, Lance and Bataille, 1991). However the mechanisms of turbulent modulation by bubbles are still unexplored, especially microstructure of the interaction between bubbles.

The objective of the present project is to elucidate the mechanism of interaction of microbubbles and microstructure of turbulence in dispersed two-phase flow. For a fundamental flow, we have examined the interaction bubble and surrounding fluid in simple shear layer, and extended to the skin friction reduction flow with higher void function. We have applied a novel technique for the measurements of velocity very close to the surface between liquid and gas phases. Digital Particle Image Velocimetry (DPIV) along with Laser Induced Fluorescence (LIF) has been developed by the author's group for velocity field measurement in the vicinity of the gas-liquid interface, and combined with Infrared Shadow Techniques (IST) for bubble shape detection.

2. Measurement Method

In order to measure the flow structure around the bubble, specifically to detect the interaction between the bubble motion and the flow field which it encounters, we implemented a Digital Particle Image Velocimetry (DPIV) system previously described by Sakakibara et al. (1993) and Tokuhiro et al. (1998). The diameter of the bubble that we measured was approximately 1000 times larger than that of tracer particles. From initial trials we noticed that the intensity of light reflected from the bubble's surface saturated the CCD device so that the intensity of light from the tracer particles was overwhelmed. And we cannot detect the tracer images in the vicinity of the bubble as shown in Figure1. Thus we applied Laser Induced Fluorescence (LIF) as fluorescent tracer particles. Methyl methacrylate ($H_2C{=}C(CH_3)COOCH_3$) with Rhodamine-B as the fluorescence dye polymerizes to give particle. We could detect fluorescence emitted by the particles through a color filter to cut the reflection into a CCD camera as shown in Figure 1. The diameter of the tracer particles is approximately 1~10 μm and a specific density is 1.02. With this set-up we could measure the flow structure in the vicinity of the bubble. In this system, image data are analyzed by cross-correlational technique, so that we can obtain the velocity vector at each location.

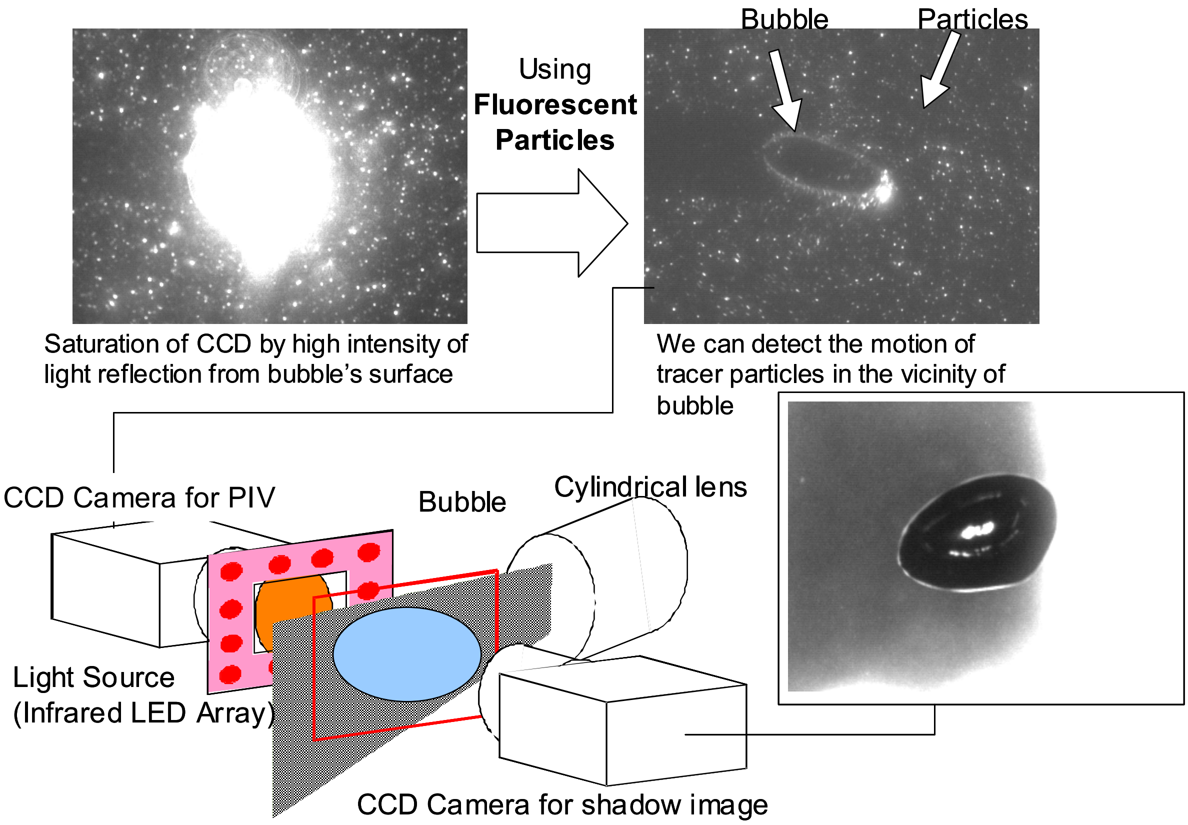

Figure 1. Typical snapshot of particle image around the bubble and schematic of measurement system.

For capturing the bubble's shape and motion simultaneously, we supplemented the DPIV-LIF system with a projection technique using infrared LEDs as the light source specifically prepared for this experiment. A bubble's image is illuminated from the back side, and imposed on a grayscale background. The bubble has been captured at one instant of a continuous oscillatory motion. The emitted light passed through a filter attached to the CCD camera and recorded the shadow and the infrared-light.

Figure 1 also depicts our arrangement consisting of two CCD cameras; one for DPIV-LIF (left camera) and the other (right) for detecting bubble shape. A square "window" array of infrared LEDs permitted a view for DPIV-LIF. In order to capture both the bubble shape and flow field simultaneously, we synchronized the triggering of the laser, the LEDs and the two CCD cameras.

3. Rinsing Bubble in a Simple Shear Layer.

One of the significant challenges in proper modeling of gas-liquid two-phase flow is the clarification of the interaction amongst various time- and length-scales describing the flow. Recently many measurement systems with image processing technique have developed and they were applied to bubbly flow (Fan and Tsuchiya, 1990, Brücker, 1998). We (Tokuhiro et. al., 1998, Tokuhiro et. al., 1999) have developed a particular technique to investigate the flow around and in the wake region of a single bubble and two similar sized air bubble confined in a downward flow of water. Of particular interest is the localized phenomena, such as the factors influencing the lift force on the bubble; that is, the interaction between gas/liquid phases and the associated transfer mechanisms.

As for the experimental apparatus it consisted of two rectangular tanks, a lower and upper, and vertical, square acrylic channel. A schematic is shown in Figure 2. In the middle of channel there is a looped belt connected to a variable speed so that we can induce a vertical shear flow between belt and the wall. We defined the region with downward flow as the test section which is 100x100mm^2 cross section area, and approximately 1000mm in length. The fluid was pumped back up to the upper tank and circulated in a manner to minimize secondary flow. At the top of the channel there is an entrance section with a honeycomb used to rectify the incoming flow. In order to tailor a stable linear shear flow we set up a grid to induced the desired shear rate. We defined the middle of the channel in span direction on the belt as the origin, downward flow direction as x-axis, and cross-sectional direction as y-axis. The laser sheet entered at z/h = 0 and illuminated a x-y plane.

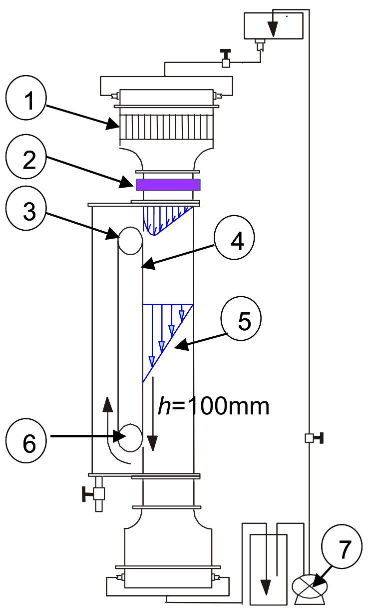

Experimental conditions

D_e[mm]	k_{avg}[s^{-1}]	Re_{rel}	Re_k	Eo	M
**8	-2.3	1330~1410	110.2	10.0	1.25×10^{-10}
**1.3	-1.9	284	2.3	0.25	1.25×10^{-10}

** 16w%Glycerin Water Solution

$$Re_{rel}=\frac{D_e U_{rel}}{\nu},\ U_{rel}=U_{bubble}-U_{fluid},\qquad Re_k=\frac{D_e^2 k_{avg}}{\nu}$$

$$Eo=\frac{gD_e^2\rho_l}{\sigma},\qquad M=\frac{g\mu_l^4}{\rho_l\sigma^3}$$

1. Honeycomb plate
2. Shear induced grid
3. Pulley
4. Belt
5. Test section
6. Motor
7. Bubble inject point
8. Pump

Figure 2 Experimental apparatus for simple shear layer flow.

Figure 3 shows the velocity vector field and vorticity color contours around the ascending bubble in time series. Each picture depicts the instantaneous flow structure. Vorticity is defined in terms of that circulation and calculated using equation ,

$$\omega_{0,0}\equiv(-u_{1,1}\Delta x-u_{0,1}\Delta x-v_{-1,1}\Delta y-v_{-1,0}\Delta y$$
$$+u_{-1,-1}\Delta x+u_{0,-1}\Delta x+v_{1,-1}\Delta y+v_{1,0}\Delta y)/(4\Delta x\Delta y)$$

Where Δx and Δy are the distance between each point of data in x, y direction. The sampling rate was approximately 23.5ms based on a limited framing rate of the CCD camera (maximum frame rate is 85 fps).

The flow structure around the bubble is shown in Figure 3. Under this condition the bubble deformed oblate ellipsoid. A vortex grew at the edge of the bubble where the shear rate was high and shed from the bubble's edge. In particular the vorticity at the right exhibits relatively higher values than the left as the bubble orients itself toward the right (from t=0sec to 47.0msec). When the relative vorticity reaches -100s^{-1}, the vortex is shed and the bubble reorients itself (at t=94.0msec).

We show the histogram of the bubble short axis orientation angle θ and several examples of bubble trajectory in each condition. In order to estimate the trajectory of the bubble, we defined the bubble's center of gravity (x_c,y_c) of the bubble's projected image, the bubble orientation angle, θ, and the orientation of the $\mathbf{U}_{rel}$, γ shown in Figure 4. This shows the examples of bubble's trajectory and Figure 5 indicates the histogram of the θ of ellipsoidal bubble. In this case the vortex shedding was occurred. In Figure 4, the arrow point at x/h=0.25 was the bubble injecting point. And the center of the amplitude of the bubble's zigzag motion passed at $x/h \geq 0.25$. It suggested that the shear flow acts on an oblate ellipsoid bubble as the force that induces bubble motion toward the direction where the relative velocity decreases (away from the belt). In Figure 5 θ was distributed -40° < $\theta \leq$ 40°. It means, bubble moved zigzag motion and also moved toward the wall. Around -20° there was one peak. The bubble was easy to orient this direction because of the shear stress induced by the vortex at the left-hand side edge; this area was easier to generate the vortex than at the right-hand side, because of the higher relative velocity at the left side in the shear layer.

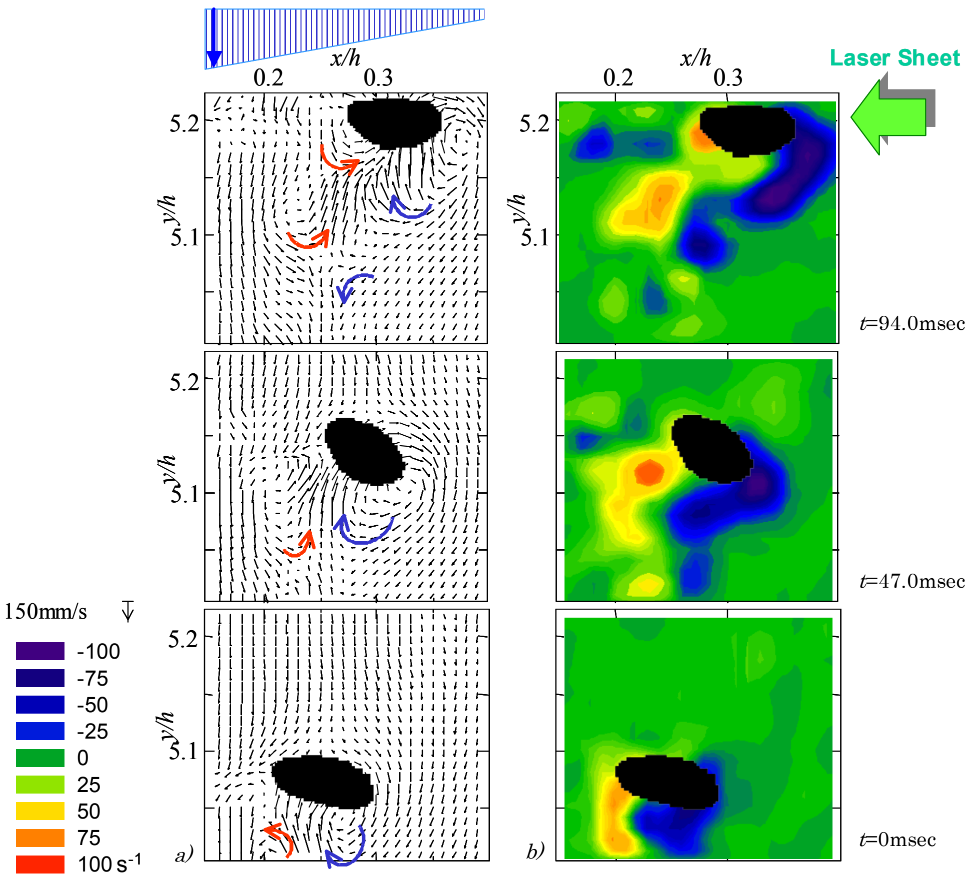

Figure 3 Instantaneous velocity vector maps and vorticity contour around a rising bubble

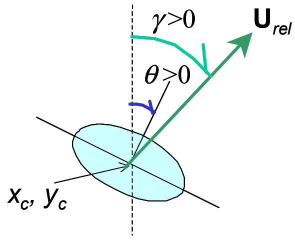

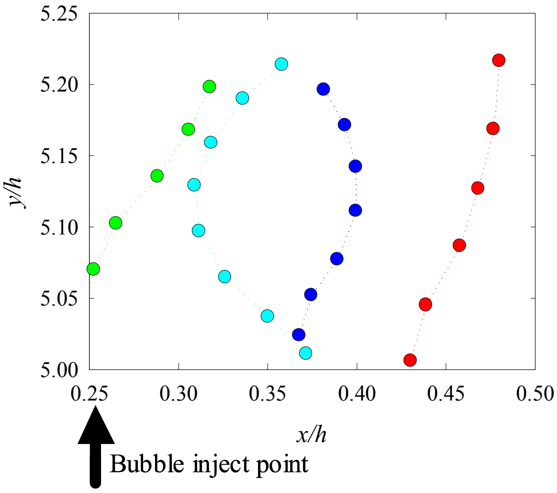

Figure 4 Trajectory of bubbles.

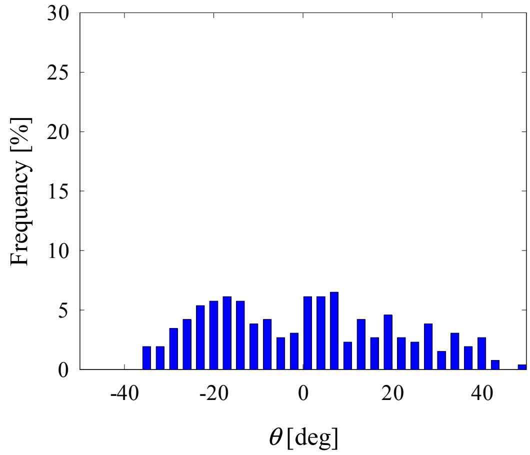

Figure 5 The histogram of the bubble orientation θ.

4. Turbulent Structure in a Upward Bubbly Channel Flow.

The objective of the experiment is to elucidate the mechanism of the interaction between bubbles in inter-particle spacing, and the influence of microscopic flow structure on the macroscopic flow structure in a fully developed channel flow. We conducted fully developed upward bubbly flow with approximately 1% of void fraction in a vertical channel. The bubble diameter was approximately 1mm. We explored the flow structure in the vicinity of bubble and also the bubble position and its shape respectively by DPIV and a shadow-image technique (Tokuhiro et al., 1998).

Figure 6 shows the schematic of experimental apparatus. As for the experimental apparatus it consisted of two rectangular tanks, a lower and upper, and vertical, square acrylic channel. Water as the fluid was pumped up to the upper tank and flow from bottom part to the top part of the channel by the water head in a manner. At the bottom of the channel there is an entrance section with a honeycomb used to rectify the incoming flow. After the nozzle there is the bubble generator. We used air as the bubbles. Figure 7 shows the schematic of the bubble generator. We used 34 sticks of stainless pipe with the inward diameter 0.07mm and outward diameter 0.50mm. The air pressure and flux was controlled by pressure gage and flow meter. Test section is the 1730mm from inlet of the channel with 50x50mm^2 cross-section area. We will define the channel width as $2h$=50mm.We defined the middle of the channel in span direction on the wall as the origin, upward flow direction as x-axis and cross-sectional direction as y-axis. The laser sheet for PIV entered at x/h=0 and illuminated an x-y plane.

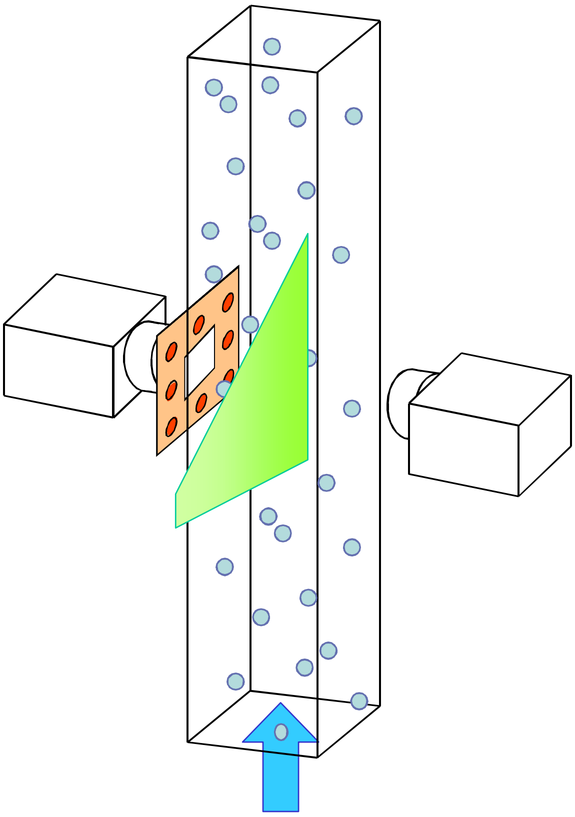

Figure 6 Experimental set up of upward bubbly flow

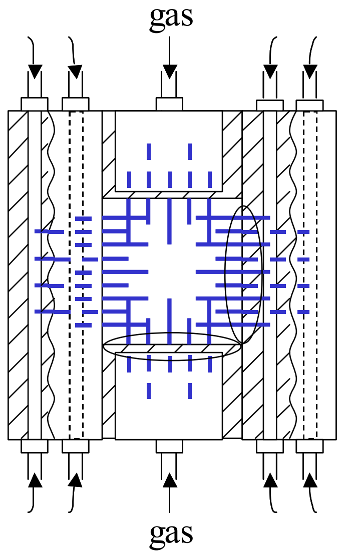

Figure 7 Microbubble generator

Figures 8 and 9 show the profile of mean streamwise velocity U_{mean}, the streamwise fluctuation velocity u_{rms} normalized by the centerline mean velocity U_{max}, in each condition. In the case of a=0.5% streamwise velocity profile was very similar to the single phase and u_{rms} increased from single phase especially at the middle of the channel and near the wall. v_{rms} also increased at the center of the channel. It suggested that the bubble disturbed the flow without acceleration the average velocity when the bubble concentration was thin.

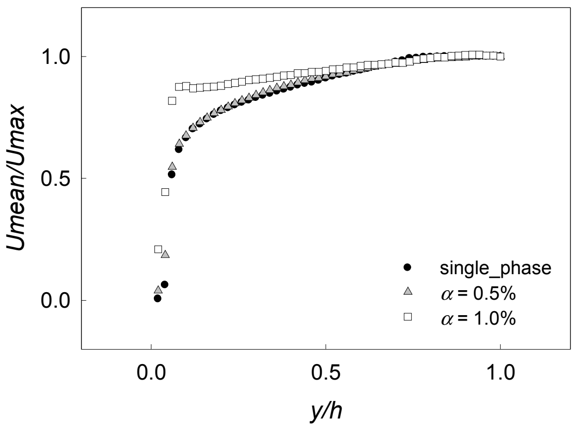

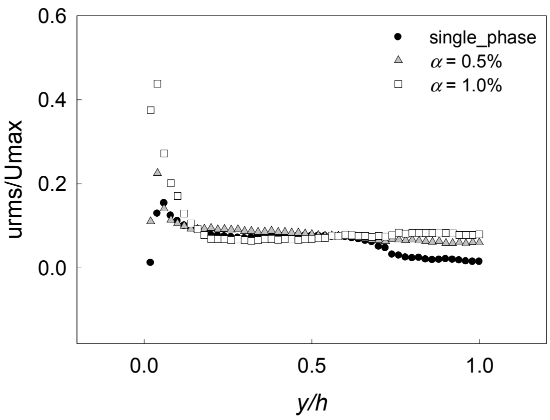

Fig.8 Profile of mean streamwise velocity of liquid-phase

Fig.9 Profiles of streamwise turbulent intensity

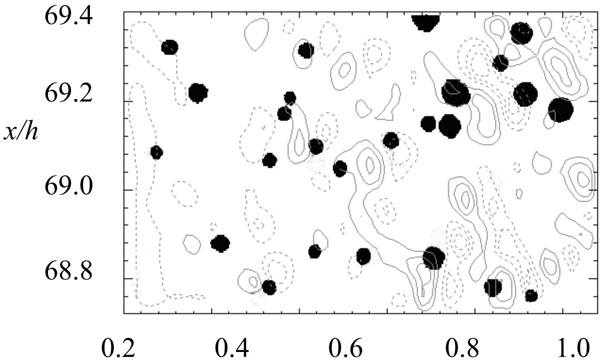

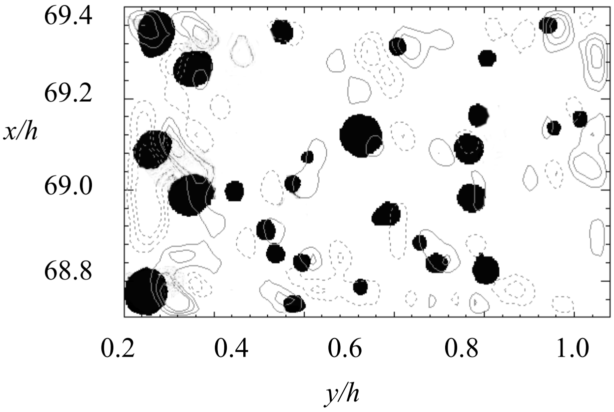

Fig. 10 Instantaneous vorticity contour (a=0.5%)

Fig.11 Instantaneous vorticity contour (a=1.0%)

Figures 10 and 11 shows the instantaneous vorticity contours. We can identify the high vorticity intensity area were appeared around the bubble especially the region of the high bubble concentration. In case of a=1.0% large bubble were ascended near the wall and high vorticity region were appeared near the wall. We noted that some vorticities were combined each other and reproduced much higher value of vorticity. It is suggested that the bubbles' wake interacted each other and the strain became high not only in the vicinity of the bubble but also in inter-particle spacing.

In the case of a=1.0% at y/h≈0.08 streamwise velocity accelerated remarkably and at the middle of the channel it decreased. u_{rms} increased near the wall and the middle of the channel. u_{rms} at y/h=0.2~0.5 was smaller than that of a=0.5%. v_{rms} increased at the middle of the channel and near the wall. This trend was very similar to the profile of u_{rms}.

5. Velocity Measurements of Microbubbles Flows for Skin Friction Reduction

Microbubbles, i.e. small bubbles injected into the boundary layer on a solid wall, reduce skin friction significantly, and have been studied intensively (e.g. Merkle and Deutch 1990) since the pioneering works by McCormick and Bhattacharyya (1973), and Bogdevich(1977). Recently several experimental studies on the mechanism of skin friction reduction by microbubbles were carried out (Kato et al. 1994, Guin et al. 1996, Takahashi et al. 1997, Kodama et.al.2000). As for the drag reduction mechanism, it is thought that the turbulent eddy inside the boundary layer is affected and that the velocity gradient at the wall becomes less so decreasing the wall shear stress, although this has not become completely clear yet.

In the present experiment, the velocity distributions in a boundary layer with microbubbles at a flow velocity of U = 5 -10 m/sec were measured by PIV (Particle Image Velocimeter). The measurements were taken for 500 mm downstream of the air injection position in a small high speed water tunnel to determine the frictional drag reduction mechanism of microbubbles. We also obtained the effect of the size of the PIV analysis area on the mean velocity measurements.

The small high speed water tunnel is shown in Figure 12. The same tunnel was established by the Ship Research Institute in 1997 as the test system for the microbubble research. The test section of the tunnel is made of transparent acrylic of 3000mm in length, 100mm in width, and 15mm in height. The flow in the tunnel can be regarded as two fully developed two dimensional boundary layers. The center of the bubble generation section is located at 1038 mm downstream of inlet of the test section The microbubble generator is shown in Figure 13. The porous plate has air holes of 2 micrometers in diameter, has a thickness of 3mm, a width of 76mm and is made from a bronze metal plate.

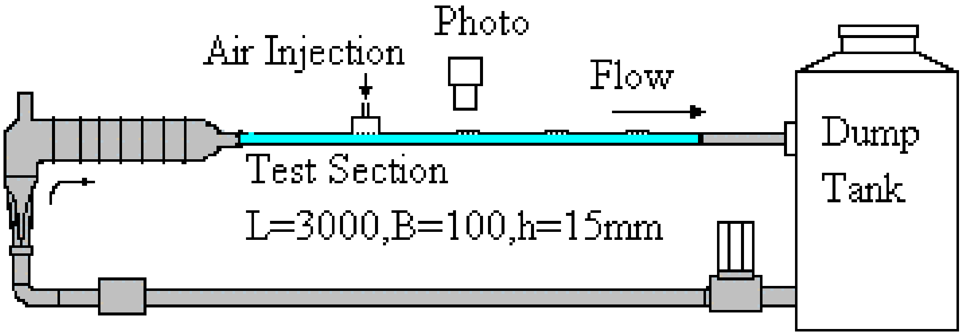

Figure 12 Circulating water tunnel for micorbubble experiments

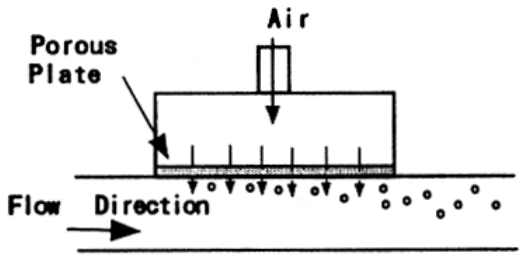

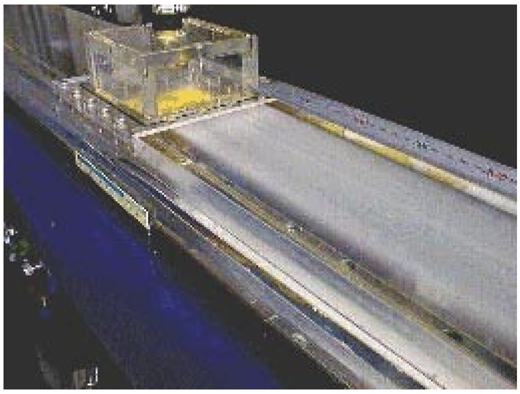

Figure 13 Air injection chamber and bubble generation through a porous plate (picture right-side)

The mean flow velocity, *U*, within the test section was found by measuring the flux of a pre-calibrated electromagnetic flow meter that was installed upstream of the test section. We describe the definition of the mean void ratio, α a, in equation.

α a=Qa/(Qa+Qw)

Qa: Air flow rate, Qw: Water flow rate = b*h*U

b: Width of the test section (100 mm), h: Height of the test section (15 mm)

U: Average speed of water

The relationship between the local frictional drag and mean void ratio is shown in Figures 14 and 15 at a flow velocity U = 5.0 and 7.0 m/sec. The vertical axis is the ratio of friction drag coefficient with microbubbles, C_f, to the friction drag coefficient without microbubbles C_{f0}, and the horizontal axis is the mean void ratio, α, within the tunnel test section. Dotted lines show an empirical formula obtained by Merkle (1990). It should be noted that the Qa values were calculated using the local pressure at each measurement location because there was non-negligible streamwise pressure gradient due to head loss in the test section. At all the speeds, the skin friction reduction increased as the amount of injected air increased. The maximum skin friction reduction was approximately 30%. It should be mentioned that Merkle's experimental data was obtained at 50mm to 65mm downstream of the point of bubble injection, and the present data was obtained at 500mm to 1500mm downstream.

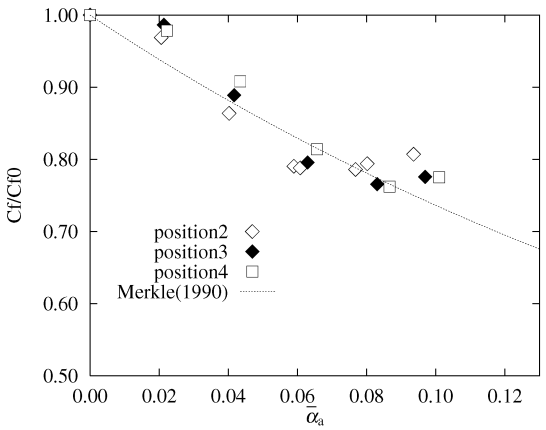

a) U = 5.0 m/s

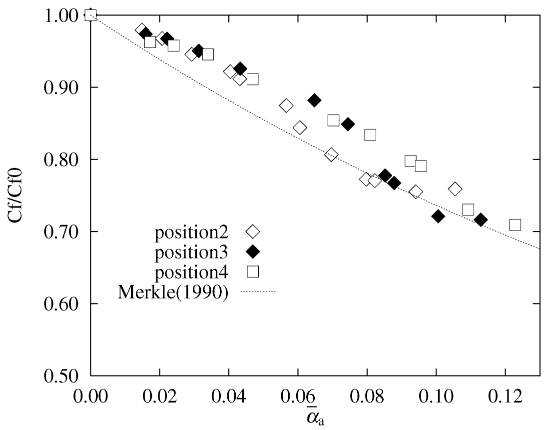

b) U = 7.0 m/s

Figure 14 Skin friction reduction as a function of void fraction.

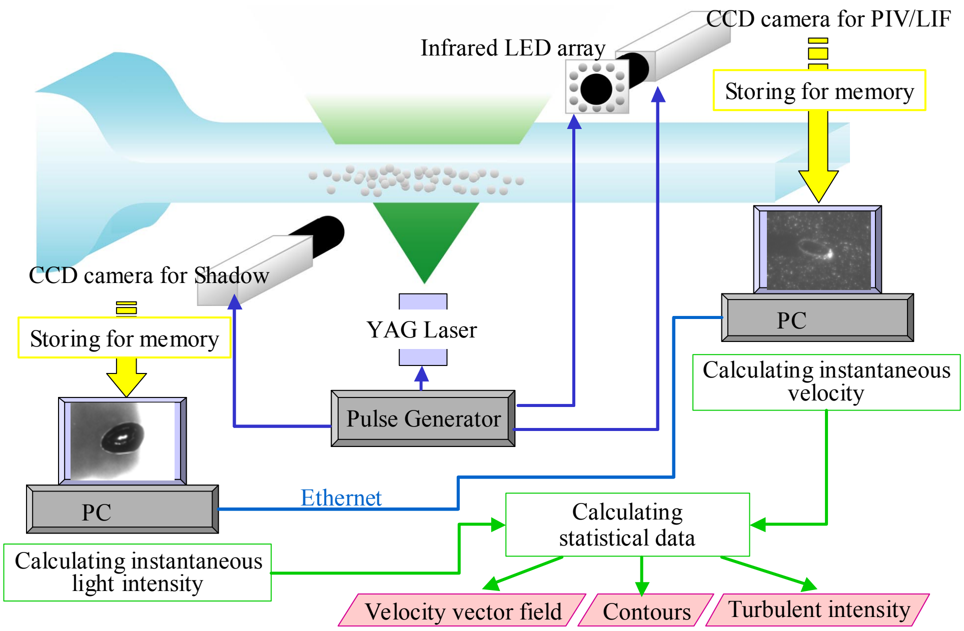

Figure 15 PIV/LIF/IST setup for a microbubble skin friction reduction flow.

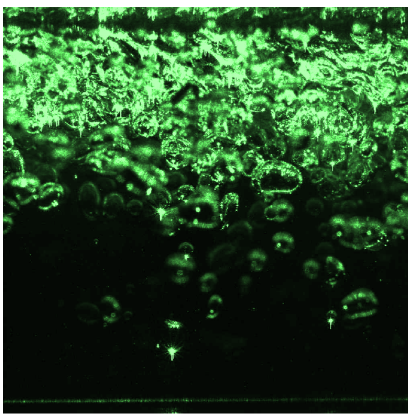

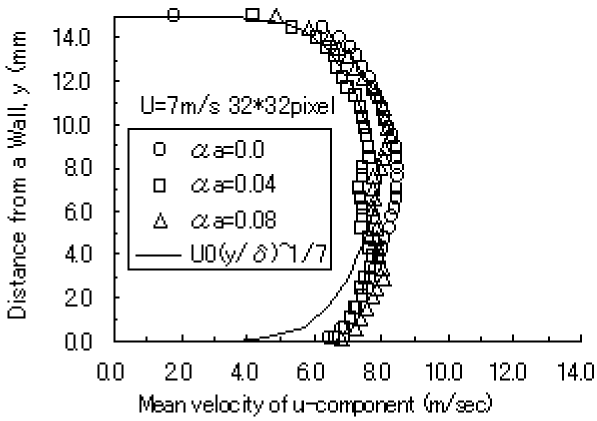

Figure 16 Flow visualization of microbubble flow and mean velocity profiles by PIV

Figure 15 indicated the up-version of PIV/LIF/IST instrumentation for high speed microbubble water tunnel flow. One example of preliminary experimental results of velocity fields are given in Figure 16.

REFERENCE

Brücker, Ch. (1998), "3-D measurement of bubble motion and wake structure in two-phase flows using scanning particle image velocimetry (3-D SPIV) and stereo-imaging", 9th International Symposium on Applications of Laser Technique to Fluid Mechanics, pp. 27.4.1-27.4.10

Clift, R., Grace, J. R. and Weber, M. E. (1978), Bubbles, Drops, and Particles, Academic Press, New York (USA).

Fan, L.-S. and Tsuchiya, K. (1990), Bubble wake dynamics in liquids and liquid-solid suspensions, Butterworth-Heinemann Series in Chemical Engineering, Boston (USA)

Guin, M.M. et al.,1996,"Reduction of Skin Friction by Microbubbles and its Relation with Near-Wall Bubble Concentration in a Channel", J. of Marine Science and Technology, Soc. Naval Arch. Japan, vol.1, No.5.

Kato, H. et al.,1994,"Frictional Drag Reduction by Injecting Bubbly Water into Turbulent Boundary Layer", Cavitation and Gas Liquid Flow in Fluid Machinery and Devices, FED-vol.190,ASME, pp185-194.

Kodama, Y., Kakugawa, A., Takahashi, T., and Kawashima, H., (2000) "Experimental study on microbubble and their application to ships for skin friction reduction", Int. J. Heat and Fluid Flow 21 pp.582-588.

Sakakibara, J., Hishida, K. and Maeda, M. (1993), "Measurement of thermally stratified pipe flow using image-processing techniques", Experiments in Fluids, Vol. 16, pp. 82-96.

Tokuhiro, A., Maekawa, M., Iizuka, K., Hihsida, K., and Maeda, M. (1998), "Turbulent flow past a bubble and ellipsoid using shadow-image and PIV techniques", International Journal of Multiphase Flow, 24, pp. 1383-1406

Tokuhiro, A., Fujiwara, A., Hihsida, K., and Maeda, M. (1999), "Measurement in the wake region of two bubbles in close proximity by combine shadow image and PIV techniques", Transaction of ASME Journal of Fluid Engineering, Vol. 121, No. 1, pp. 191-197

Lance, M., and Bataille, J. (1991) ,"Turbulence in the liquid phase of a uniform bubbly air-water flow", Journal of Fluid Mechanics, Vol. 222, pp. 95-118.

McCormick, M.E. and Bhattacharyya, R., 1973, "Drag Reduction of a Submersible Hull by Electrolysis", Naval Engineers Journal, Vol.85, No.2, pp. 11-16.

Merkle, C. and Deutsch, S.,1990,"Drag Reduction in Liquid Boundary Layers by Gas Injection", Progress in Astronautics and Aeronautics vol.123, AIAA, pp.351-412.

Theofanous, T. G., and Sullivan, J. (1982), "Turbulence in two-phase dispersed flows", Journal of Fluid Mechanics, Vol. 116, pp. 343-362

Serizawa, A., Kataoka, I., and Michiyoshi, I. (1975), "Turbulence structure of air-water bubbly flow. II. Local properties", International Journal of Multiphase Flow, Vol. 2, No. 3, pp.235-246

Takahashi,T. et al.,1997,"Streamwise Distribution of the Skin Friction Reduction by Microbubbles", J. of the Society of Naval Architects of Japan, vol.182, pp.1-8.

Takahashi, T. et al.,1999,"Experimental skin friction reduction by microbubbles using a ship with a flat bottom", Turbulence Symposium, Tokyo.

Watanabe, O. et al.,1998,"Measurements of Drag Reduction by Microbubbles Using Very Long Ship Models", J. of Soc. Naval Architects, Japan, vol.183, pp.53-63.